

Efficacy of Electrical Resistivity Imaging Technique in Mapping Bedrock in Some Regions of South Iraq

Nadia Ahmed Aziz Zaidoon Taha Abdulrazzaq Hayder Abdul Zahrah Alwan
 Ministry of Science and Technology/ Space Directorate and Communication-
 Geophysics Researches Center
 Baghdad-Iraq
 E-mail: nadia_naa@yahoo.com

Abstract

Two-dimensional (2D) electrical resistivity imaging (ERI) method was used to detect the contact between sediment and bedrock some regions of south Iraq. ABEM Terrameter LS used for data collection, using three 2D electrical resistivity profiles. For the fieldwork, two-dimensional surveying carried out along three profiles using Dipole-dipole array with 8 m electrode spacing. The maximum depth of investigation was 50 m.

The data analyzed and explained 2D inversions by the RES2DINV software. The obtained data analyzed, and 2D models of the subsurface generated. The resistivity data were inverted into subsurface electrical sections using the least-squares inversion technique. Then, the contact between the bedrock and sediment was observed. Our results indicate well-defined boundary in the resistivity structure that can be used to estimate the quantity of sediments covering bedrock.

Keyword: Geo-electrical, Resistivity, 2D Inversion, Bedrock, and Subsurface Mapping.

كفاءة تقنية تصوير المقاومة الكهربائية في الطبقة الأساس في بعض مناطق جنوب العراق

نادية احمد عزيز زيدون طه عبد الرزاق حيدر عبد الزهرة علوان
 وزارة العلوم والتكنولوجيا/ دائرة الفضاء والاتصالات - مركز بحوث الجيوفيزياء
 بغداد-العراق

الخلاصة

استخدمت تقنية التصوير المقاومة الكهربائية ثنائي الأبعاد لتحديد الطبقة الأساس لبعض مناطق جنوب العراق باستخدام جهاز (ABEM Terrameter LS) لجمع البيانات وبطريقة Dipole-dipole لمسح المقاطع الطولية ثنائية الأبعاد وبمسافة 8 م بين قطب واخر وكان اقصى عمق للاختراق 50 متر. مسحت ثلاثة مقاطع طولية للمقاومة الكهربائية ثنائية الأبعاد.

حللت وفسرت البيانات ثنائية الأبعاد بواسطة برنامج RES2DINV لاعداد النموذج ثنائي الأبعاد لتحت الارض. استخدمت تقنية المربعات الصغرى لتفسير البيانات ولرسم الموديل النهائي وتفسيره ومن ثم حدد الحد الفاصل بين الرواسب والطبقة الصخرية الصلبة. اظهرت النتائج وجود حدود واضحة المعالم في قيم المقاومة والتي تم عن طريقها تحديد الحد الفاصل فضلاً عن تقدير كمية الرواسب الواقعة فوق الطبقة الصخرية الصلبة.

الكلمات المفتاحية: جيوكهربائية، المقاومة، عكس البيانات ثنائية البعد، الطبقة الأساس و رسم الخرائط التحت السطحية.

Introduction

Electrical resistivity techniques have been used to determine the location of various geologic and soil strata, bedrock fractures, faults, and voids. In the earlier applications, the technique was considered to be very labour intensive. The development of the 2D multi-electrode surveys has been able to reduce this aspect of the survey (Heather *et al.*, 1999).

Bedrock can be define as a solid rock that underlies loose material, such as soil, sand, clay, or gravel.

Many works have been done to establish a relationship between soil engineering test and ERI data (Israil and Pachauri, 2003; Cosenza *et al.*, 2006; Gay *et al.*, 2006). Another important advantage of ERI is that it produces continuous information of the subsurface and probes into several meters below the surface. Survey design and layout strategies that produce optimum information using different Electrical Resistivity Imaging (ERI) configurations and set up in different geological settings have been the topic of several studies (Alumbaugh and Newman, 1999; Stummer *et al.*, 2004; Ayolabi *et al.*, 2009).

2D electrical resistivity imaging survey is produced by injecting current into the ground through two current electrodes and measuring the resulting voltage difference at two potential electrodes. This process is repeated for many current/potential electrode configurations to produce a pseudo-section of apparent resistivity. The resultant data are then processed using a 2D inversion. Variations in the underlying sediment or rock units indicated by different electrical resistivities can then be observed as strong gradients in resistivity. Although the subsurface resistivity distribution could then be interpreted and mapped by eye, we will show that this subjective method should be done with caution because of the diffusive nature of the

electrical field. This paper aims at defining a better location of the electrical interface between a high-resistivity layer and a low-resistivity layer, like the bedrock–sediment contact (Marr and Hildreth, 1980; Vafidis *et al.*, 2005).

The most commonly used arrays in the 2D electrical imaging surveys are conventional arrays such as the Wenner, Schlumberger or dipole-dipole arrays. These arrays are often well understood in terms of their depths of investigations, lateral and vertical resolution and signal- to- noise ratios (Al Fouzan, 2008).The Dipole-dipole array gives good horizontal resolution, while the Wenner and Schlumberger arrays are more intended for vertical resolution. In the application to karst surveys, the dipole-dipole array has provided highest precision of ground changes sensitivity and has the greatest sensitivity to vertical resistivity boundaries (Zhou *et al.*, 2002).

The electrical profiles were interpreted using the RES2DINV resistivity software. This calculation program is based on the least-square method with an enforced smoothness constraint, modified with the quasi-Newton optimization technique. The inversion method constructs a model of the subsoil using rectangular prisms and determines the resistivity value for each of them, minimizing the differences between the observed and calculated apparent resistivity values (Loke and Barker, 1996; Loke and Dahlin, 2002).

The goal of the present work aimed to investigate the efficiency of 2D of electrical resistivity imaging technique in mapping bedrock.

Materials and Methods

Geology of the Studied Area

Dibdibba Formation (Pliocene-Pleistocene)

The formation consists of conglomeritic sandstone and claystone, intermdlded by pebbly sandstone layers, occasionally contains vertebrate bones. These

beds overlain by pebbly calcareous sandstone partly micaceous.

The sandstone is whitish grey, massive. The conglomerate is composed of gravel size: sandstone, claystone fragments (in the lower part); detrital carbonate fragments, quartz and igneous rocks fragments.

Generally, the thickness increases southwards. The exposed thickness ranges from 2m to 9m.

The formation covered uncomfortably by Quaternary deposits such as sand sheet deposits and sand dune deposits (Hassan *et al.*, 2002).

Quaternary

The Quaternary sediment has a huge area extent covering. These sediments are of Pleistocene and Holocene ages and were deposited by fluvial, eolian and lacustrine agencies (Hassan *et al.*, 1989).

They were composed of various types of sediment which originated mostly by eolian and rain-wash processes; they were mixture of various fragments, clayey, silty and sandy, also with admixture of gravels, they were mostly calcareous, gypsums, sometimes compacted, friable and jointed with gypsum veins.

Study and Survey Design

Three profiles were measured namely line A, B and C. Dipole-dipole array was used for all profiles to get better depth penetration in the outer parts of the survey area. The electrode spacing was 8 meters.

A general 2D profile acquisition of the resistivity data was fairly straightforward. The data processed and inverted using RES2DINV software. The program generates the inverted

resistivity-depth image for each profile line.

Results and Discussion

Line A

The resistivity values for this line vary between 5 and 1101 ohm.m, the total length was 320 m, the depth of investigation 50 m, and the RMS was 2.5% after 5 iterations (Fig. 1).

The inversion resistivity image shows three different layers, the first layer contains quaternary deposits showing high resistivity that ranges from 518 to 1101 ohm.m. The resistivity values for the intermediate layer was 115 ohm.m, which may represent Debdibba Formation. The third layer shows low resistivity value (5-25 ohm.m) and was interpreted as an unconfined aquifer.

In this section, the separation between the sediment and the bedrock was appear at depth 6.2 m.

Electrical Resistivity technique proved to be versatile, fast in delineating aquifers and mapping shallow subsurface anomalies. It had a wide flexibility in covering large data with dense sampling for a given block of rock mass and at the same time intelligent in acquiring different strength of signals from the subsurface geological characteristics. The true resistivity models resulted from mathematical computation, standard and advanced inversion approaches in conjunction with the measured apparent resistivities had been helpful in resolving the geological formations, depth of bedrock, and the groundwater in different geological terrains with much more confidence and with high resolution as compared to conventional resistivity methods. The essence of this unique technique is seen and proved worth in the present day geo-scientific study.

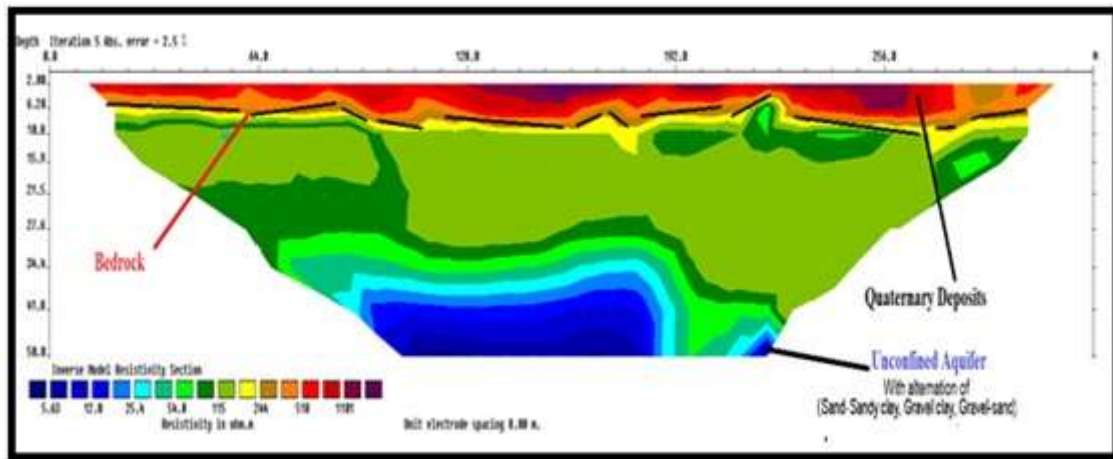


Fig. (1) Inverted Resistivity Section for Line A.

Line B

The inversion result of this line was shown in Figure 2. The resistivity values ranged between 3 and 953 ohm.m. The RMS 3.28 % after 5 iterations. The length of this spread line is 320 m with maximum depth of investigation 49.9 m. The surface uppermost layer showed relatively high resistivity values ranging from 424 to 953 ohm.m which it is quaternary deposits, with an inhomogeneous resistivity distribution which could be explained by the variable

water content levels within the same layer. To the lower, a low resistivity area (with green color) with a value 83 ohm.m may be interpreted as Debdibba Formation. The third layer shows low resistivity value 7 ohm.m and was interpreted as an unconfined aquifer. In this section, the separation between the sediment and the bedrock was appear at depth 7 m.

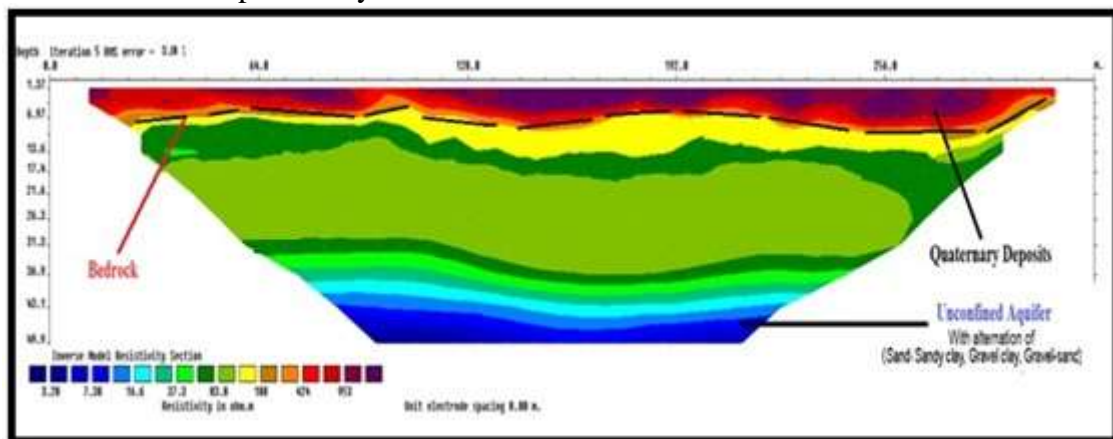


Fig. (2) Inverted Resistivity Section for Line B.

Line C

The 2D inversion resistivity pseudo-section of Line C (Fig. 3) trends from W to E direction, the total length of survey line was 320 m, and the maximum depth of investigation was 50 m. The resistivity values vary from 2 to 795 ohm.m with RMS 4.5% after 5 iteration.

In this section, the separation between the sediment and the bedrock was appear at depth 10 m.

The subsurface resistivity image along Line C appears basically identical to that obtained from Line A and Line B, with the same layers appeared.

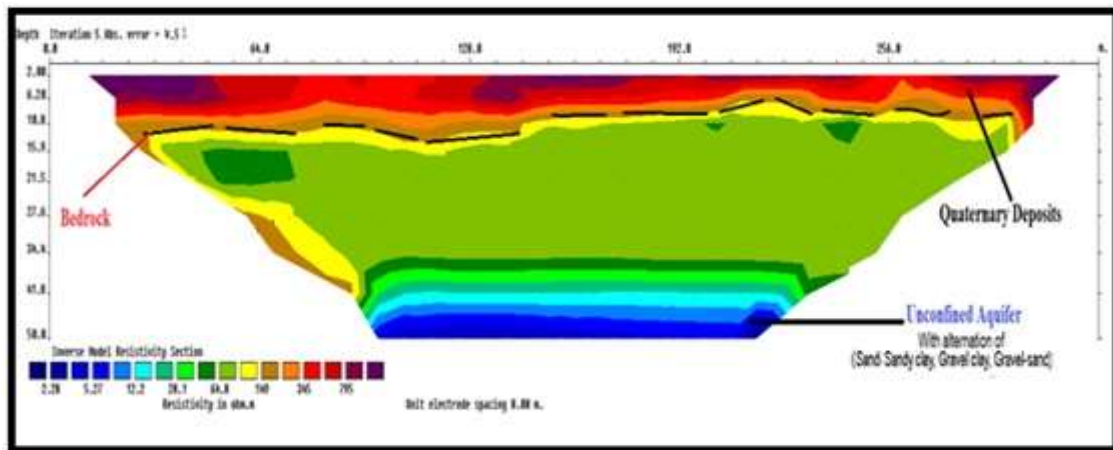


Fig. (3) Inverted Resistivity Section for Line C.

Conclusion

The results showed a consistent distribution in all 2D ERI profiles, where a shallow high resistivity zone (interpreted to be Quaternary deposits) covers a low-resistivity zone (interpreted to be bedrock). Apparently, resistivity of the sediment follows a log-normal distribution with an average of about 345 ohm.m. The broad distribution of resistivity in these sediments is likely influenced by randomness associated with grain size, pore space, and level of water saturation.

Electrical resistivity is non-destructive and can provide continuous measurements over a large range of scales. Besides, it is an attractive method for soil characterization in the contrary to regular drilling which perturbs the soil.

It is found that Dipole-dipole array is a suitable choice to be considered and used for such investigation as it is suitable for field conditions; provides high signal strength and provides adequate penetration depth.

The ability of geo-electrical imaging to indicate changes in rock conditions by means of varying resistivity makes it a valuable tool in the pre-investigation.

References

AL Fouzan, F.A. (2008) Optimization Strategies of Electrode Arrays Used in Numerical and Field 2D Resistivity

Imaging Surveys, PhD. thesis, Universiti Sains Malaysia, 25-48.

Alumbaugh, D.L. and Newman, G.A. (1999) Image Appraisal for 2-D and 3-D Electromagnetic Inversion, In: Proceedings of the Society of Exploration Geophysicists Annual Meeting, New Orleans, 1998. New Orleans, Louisiana, The Society of Exploration Geophysicists, 2–10.

Ayolabi, E.A.; Folorunso, A. F.; Adeoti, L.; Matthew, S. and Atakpo, E.(2009) 2-D and 3-D Electrical Resistivity Tomography and Its Implications, A Paper Presented at the 4th Annual Research Conference and Fair Held at the University of Lagos, Akoka, 8th Jan, 2009, p189. www.ivsl.org.

Cosenza, P.; Marmet, E.; Rejiba, Y.; Tabbagh A. and Charlery, Y. (2006) Correlations between Geotechnical and Electrical Data: A Case Study of Garchy In France, Journal of Applied Geophysics, 60, 165-178.

Gay, D. A.; Morgan, F. D.; Vichabian, Y.; Sogade, J. A.; Reppert, P. and Wharton, A. E. (2006) Investigations of Andesitic Volcanic Debris Terrains: Part 2 – Geotechnical, Geophysics, 71, B9–B15.

Hassan, H.A.; Ismail, S.K and Al Dabbas, M. (1989) Regional hydrogeological Condition of Dibdiba Basin Southern Iraq. J.Agric. Water Resal. Res, 8 (1),167-180.

Hassan, K.M.; Al-Khateeb, A.A.G.; Khlaif, H.O.; Kadhum, M.A. and Saeed, F.S. (2002) Detailed Geological Survey for Mineral Exploration in Karbala – Najaf Area. Part 1, Geology. GEOSURV, Int. Rep. 2874.

Heather, L.; Stahl, A.; Leberfinger, L. and Warren, J. (1999) Electrical Imaging: A Method for Identifying Potential Collapse and other Karst Features Near Roadways. Science Applications International Corporation, Middletown Pennsylvania, USA.

Israil, M. and Pachauri, A.K. (2003) Geophysical Characterization of a Land Slide Site in the Himalayan Foothill Region, Journal of Asian Earth Sciences, 22, 253-263.

Kearey, P.; Brooks, M.; and Hill, I. (2002) An Introduction to Geophysical Exploration, Blackwell Science, Oxford.

Loke, M.H. (2012) Tutorial: 2D and 3D Electrical Imaging. <http://www.georentals.co.uk/Lokenote.pdf>.

Loke, M.H. and Barker, R.D. (1996) Rapid Least-squares Inversion of Apparent Resistivity Pseudosections by **Marr, D. and Hildreth, E.** (1980) Theory of Edge Detection. Proc. R. Soc. Lond., B 207, 187–217.

Stummer, P.; Maurer, H. and Green, A.G. (2004) Experimental Design:

Electrical Resistivity Data Sets That Provide Optimum Subsurface Information, Geophysics, 69 (1), 120–139.

U.S. Army Corps of Engineers (1995) Engineer Manual 1110-1-1802, CECW-EG, Department of the Army, Washington, DC 20314-1000.

Vafidis, A.; Economou, N.; Ganiatsos, Y.; Manakou, M.; Poulioudis, G.; Sourlas, G.; Vrontaki, E.; Sarris, A.; Guy, M. and Kalpaxis, Th. (2005) [Integrated Geophysical Studies At Ancient Itanos \(Greece\). J. Archaeol. Sci. 32, 1023–1036.](#)

Zhou, W.; Beck, B.F. and Adams, A.L. (2002) [Effective Electrode Array in Mapping Karst Hazards in Electrical Resistivity Tomography. Environmental Geology 42, 922–928.](#)

Loke, M.H. and barker , R.D. (1996) [Raped Least – Squares Irver Sion of Apparent Resis tivity pseudosechons by a Quasi-Newton Method. Geophys Prospect 44,131–152.](#)

Loke, M.H. and Dahlin, T. (2002) [A comparison of the Gauss-Newton and Quasi-Newton Methods in Resistivity Imaging Inversion, Journal of Applied Geophysics, 49, 149–162.](#)

Milson, J. (2003) Field Geophysics”, 3rd Edition, John Wiley and Sons Ltd, 232.